Experiment with Stored 0.7-MeV Ions: Observation of Stability Properties of a Nonthermal Plasma

D. Al Salameh,[a] S. Channon, B. R. Cheo,[a] R. Leverton, B . C. Maglich, S. Menasian, R. A. Miller, J. Nering, and C. Y. Wu[b]
Aneutronic Energy Laboratory, United Sciences, Inc., Princeton, New Jersey 08540
(Received 9 November 1983)

A large-orbit, nonthermal d^+ migma plasma with $P_\theta \sim 0$ and $E_{\text{ion}} = 0.7$ MeV was formed in the center of a simple mirror with densities $n = 10^9$–10^{10} cm^{-3}. Confinement time was 20–45 s. Flute, negative-mass, and ion-cyclotron instabilities, found in other mirrors at several orders-of-magnitude lower n, were not observed. An instability was suppressed by an electric field. Confinement parameters are $E_i n_c \tau \sim 10^{14}$ keV cm^{-3} s, $n_c\tau \sim 10^{11}$ cm^{-3} s, luminosity $\sim 10^{29}$ cm^{-2} s^{-1}.

PACS numbers: 52.55.Jd, 29.20.Dh, 52.35.Py

Simple magnetic mirrors have been abandoned for the confinement of thermalized plasmas because the negative-mass,[1,2] flute,[3-5] ion-cyclotron,[6] and Harris[2] instabilities limited hot-ion densities to $\sim 10^8$ cm^{-3}. We have increased the volume average and central plasma densities to $n_v \sim 10^9$ and $n_c \sim 10^{10}$ cm^{-3}, respectively, to investigate stability[5,7-9] against these effects of a special case of nonthermal plasma referred to as the migma plasma.[10-12] Migma is characterized by (1) large Larmor-radius orbits, $r_L \sim \frac{1}{2}R$, R equals the plasma radius; (2) small canonical angular momentum, $P_\theta \sim 0$, giving a centrally peaked radial-density distribution[11]; (3) non-Maxwellian, peaked distribution of ion energies, E_i; and (4) a large ratio $(E_i/T_e) \sim 10^3$, with $E_i = 650 \pm 100$ keV and electron temperature $T_e = 0.4 \pm 0.3$ keV. The plasma volume, $V = 135$–400 cm^3, was a disk of $R = 9.3 \pm 0.1$ cm and height $Z_0 = 1 \pm 0.5$ cm. The physics regime was given by the plasma-to-cyclotron frequency ratios $0.2 < \omega_{pi}/\omega_{ci} < 0.5$ and $13 < \omega_{pe}/\omega_{ci} < 27$ for ions and electrons, respectively, where an unstable gap against $m = 1$ flute was predicted.[4,12]

The vacuum system of the early experimental setup[11] (in which $n_v \sim 10^8$ and $n_c \sim 10^9$) has been improved[13] to enable injection of a 0.5-mA dc beam of 1.45-MeV $D_2{}^+$ while maintaining $p = 3 \times 10^{-9}$ Torr (Fig. 1). Plasma was formed by collisional dissociation of $D_2{}^+$'s near the center of symmetry of the magnetic field $B_0 = 3.17$ T. The beam could be cut off in 1 ms to measure the ion confinement time, τ. The trapped d^+'s travel in precessing, quasicircular orbits of rosette pattern.[10] For each orbit the distance of closest approach to C is referred to as the impact parameter b. There are three characteristic ion frequencies of migma orbits: radial, precessional, and axial, $\omega_r \simeq 23$, $\omega_P \simeq 0.9$, and $\omega_z \simeq 8$ MHz, respectively. (In thermal plasma only $\omega_r \neq 0$.) Amplitude of axial oscillations was typically $z_0 \simeq 0.5$ cm. Three nondestructive diagnostics were used: (1) An rf pickup system[11,14] yields the number of trapped ions N, at any time and, consequently, τ. Schottky noise produced at frequency ω is picked up on a pair of plates of radius $\frac{1}{3}R$ placed at $Z = +4$ and -4 cm. The observables are frequency-power spectra $P_r(\omega)$ and $P_z(\omega)$, where r and z refer to radial (common mode) and axial (differential). The distribution in b is calculated from P_r. $\langle z_0^2 \rangle$ is inferred from P_z. A variable dc bias, U, up to ± 1.0 kV, can be applied on each of the pickup plates. (2) A charge-exchange neutral detector[11,15] (CEND) measured the number and energy of neutralized deuterium atoms to obtain N, E_i, and the ion energy-loss rate dE_i/dt (Fig. 2). (3) A nuclear-particle-detector system[11,15] measured the proton and triton rate and energy from the D(d,p)T reaction and distinguished p's produced in fast+fast ($d^+ + d^+$) reactions from those from fast+slow ($d^+ + D^0$ gas) reactions. No T_e diagnostic was installed; the range of T_e was inferred[16] from the rf system's response to change of U.

Distributions in b were sharply peaked at $b = -1.4$ cm with a full width at half maximum of 0.4 cm, similar to Fig. 3 in Ref. 11. Figure 3 shows the scope trace of the P_z amplitude—which is proportional to N—for a wide frequency band, $\Delta\omega$ (all trapped ions), with $U = 0.3$ kV. With $U = 0$ (not shown) P_z increased linearly with time until $N = 5 \times 10^{10}$ was reached. Above this, intense bursts of rf activity occurred and the sharp peak in b distribution was greatly attenuated. The burst-signal spectrum was similar to that of the Harris instability,[2] but while one expects[6] the dominant frequency ω_z with sidebands of ω_r we have found sidebands of $(\omega_r + 2n\omega_p)$. When, by trial and error, a stabilizing U was found, an order-of-magnitude higher N was reached (peak in Fig. 3). With instabilities suppressed, τ was measured from decaying $P_r(\omega)$ following beam cutoff. With $U = -1$ kV, τ was exponential; with $U = 0$, its slope increased with time. The maximum observed N was $(3.2 \pm 0.5) \times 10^{11}$, with $\tau = 20$ s, and ion energy-loss rate of $dE_i/dt = -2$ keV/s. For $N = 10^{10}$, $\tau = 45$ s was measured. Our confidence that the rf signals were incoherent has been derived from four observations: (i) Each measurement was carried out with both wide and

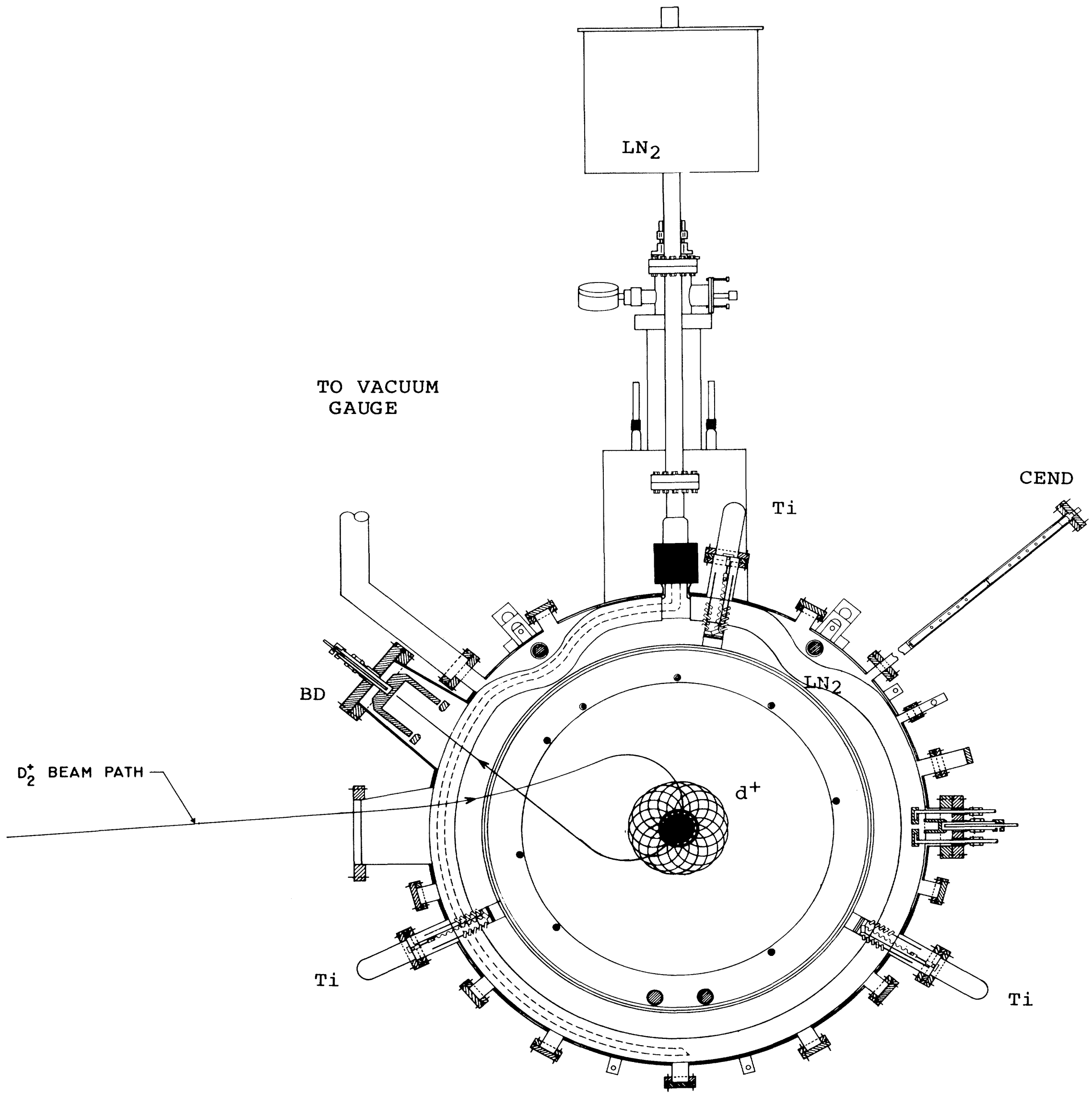

FIG. 1. Cross-sectional drawing through $z=0$ plane of the chamber. CEND, charge-exchange neutral detector; Ti, titanium sublimator pumps; LN_2, liquid N_2;d^+, orbits of trapped d^+ ions; C, center of symmetry $x=y=z=0$; BD, beam dump.

narrow $\Delta\omega$, giving the same N independent of the frequency. When $\Delta\omega$ was reduced tenfold, the $P(\omega)$ decreased tenfold. (ii) We were able to produce a coherent signal by driving the orbits into negative-mass instability and are familiar with its features. The rf spectrum itself showed no evidence of coherence; there were no spikes or narrow peaking—except when passing through the region of the (presumed) Harris instability, but no measurement of P_z from that region was used. (iii) Nuclear particle detection: The N deduced from the proton counting rate agreed to within 20% with that obtained from rf measurements. The nuclear reaction rates between plasma ions and $D_2{}^0$ was unaffected by the cutting off of the injected $D_2{}^+$ beam. The proton energy spectrum was as should be expected (Fig. 4). (iv) CEND: The *neutral* -particle counting rate from CEND indicated somewhat (30%–50%) lower value of N than either the rf or nuclear particle detectors; this was due to a misalignment of the CEND with the midplane of the stored migma—a contributing factor to P_z which may add or substract from the N would be electron effects. We estimated an upper limit of $+3$ dB as a result of this, which was subtracted out in each reading. Hence, our N values are conservative.

In obtaining n from N, uncertainty arises from es-

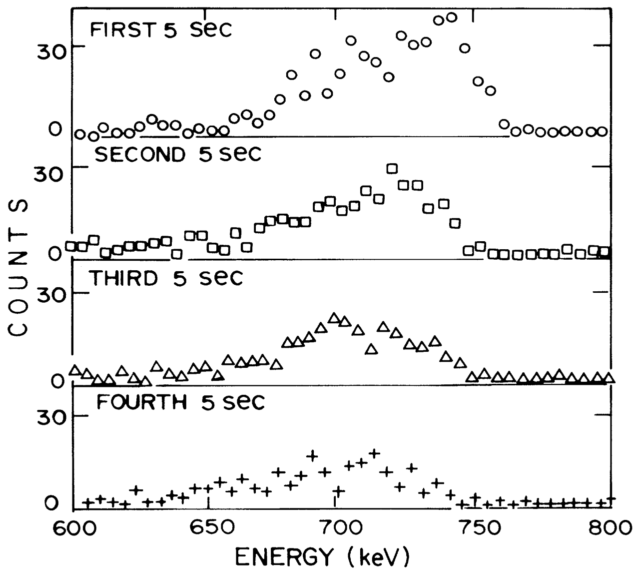

FIG. 2. Charge-exchange spectrum sequence: four spectra acquired in four intervals during ion-number decay with $U = -220$ V, showing $dE_i/dt = -2$ keV/s.

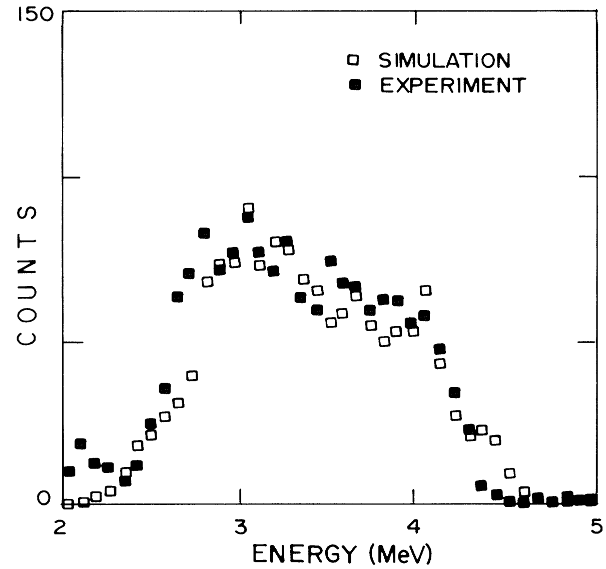

FIG. 4. Observed proton spectrum (closed squares) compared with its simulation from D(d,p)T reactions between two fast d^+'s and a fast d^+ and D_2 gas (open squares).

timating Z_0 (not measureable at higher n as a result of electron z motion). At low n, where the effect is negligible, we measured $\langle Z_0 \rangle = 0.5 \pm 0.15$ cm. Assuming multiple scattering (MCS) the only broadening mechanism,[17] we obtain $h \geqslant 0.6$ cm, $n_v \leqslant 2\times 10^9$ cm^{-3}, and $n_c \leqslant 10^{10}$ cm^{-3}. Defining a "central fast-ion density," $n_{\rm cfi}$, as the average over a disk of radius R and 1 Debye length (0.1 cm) thick, we find $1.5\times 10^9 < n_{\rm cfi} \leqslant 5\times 10^9$ cm^{-3}. The confinement parameters were as follows: $E_i n_c \tau \simeq 3\times 10^{14}$ keV cm^{-3} s, $n_c\tau \simeq 4\times 10^{11}$ cm^{-3} s, and luminosity $L = I/\sigma \simeq 2\times 10^{29}$ cm^{-2} s^{-1}, with I and σ given in Ref. 10.

The negative-mass instability threshold in DCX-1 was $n_{\rm cfi} = 5\times 10^5$ cm^{-3}; even for larger r_L, there were large losses.[1,2] With near-axis injection ($P_\theta \sim 0$), we find *stability against negative mass*[9] up to the highest density reached. This instability was deliberately produced by steering the beam into concentric orbit, $b = -r_L$, i.e., $P_\theta =$ large. We used the sharp and

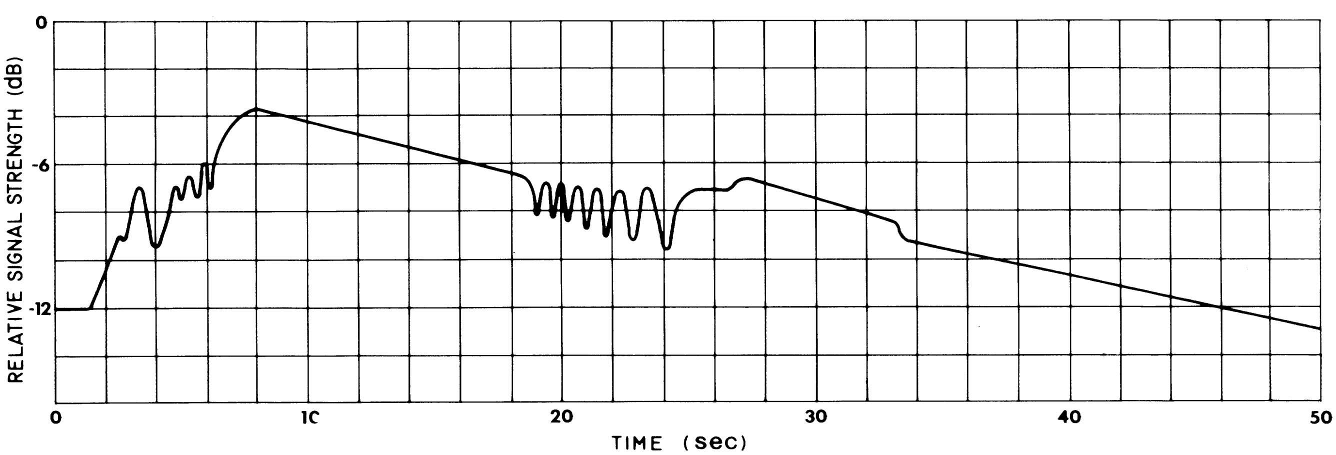

FIG. 3. Composite tracing of multiple-exposure ion buildup and decay curves showing onset of instability at -10 dB during filling; stable confinement above -6 dB; stable, nearly exponential decay to -6.5 dB; and unstable decay to -9 dB followed by stable decay. $U = -225$ V was applied to allow passage through the unstable zone. Signal strength after 24 s was affected by contributions from electrons (observed up to 3 dB with trapping bias applied); all reported N and n results with $U \neq 0$ have been reduced by a factor of 2 to allow for this effect.

TABLE I. Parameters achieved in this experiment and in DCX-1.

	This experiment	DCX-1
Ion species	d^+	p^+
Ave. ion energy (keV)	700	300
Maximum central fast ion density $n_{\rm cfi}$ (cm^{-3})	$(3\pm2)\times10^9$	2×10^8
τ at maximum $n_{\rm cfi}$ (s)	20 ± 5	60
Triple product $Tn_{\rm cfi}\tau$ (keV cm^{-3}s)	4×10^{13}	2.5×10^{12}
Neg. mass instability threshold $n_{\rm cfi}$ (cm^{-3})	not observed	$(3\text{–}5)\times10^5$
Number of stored ions N	$(3.2\pm5)\times10^{11}$	
Central density n_c (cm^{-3})	10^{10}	

reproducible transition to the negative-mass instability for calibration of B_0. Previous experiments with small r_L observed flute instabilities at $n_v \sim 10^7$ cm^{-3}. We observed *no flute instability;* this is consistent with DCX-1 experience and the trend of large-r_L measurements[5] in the Phoenix II device, which achieved $n_e = 2\times10^{10}$ cm^{-3}. However, the hot-ion component in Phoenix was only 15%, the remainder being the cold, ionized background gas. Even this density was reached only when stabilizing multipole fields were added; without them, the flute limited[18] the density to 3×10^8 cm^{-3}. Hence, our results can be compared only with those of DCX-1 (Table I). The ion-cyclotron instability[6] was not seen.

The τ values observed after cutting the beam off were consistent with charge-exchange ion loss and exponential decay. The observed dE_i/dt is consistent with about equal participation of the ionization loss in gas and electron drag.[19,20] However, the buildup behavior was only initially exponential; saturation was reached somewhat below the MCS limit $n \simeq 10^{11}$. This could have been caused by either incomplete neutralization (space-charge effects and/or single-particle resonances) or by very cold electrons, or both. Electron cyclotron heating would show if the cured instability was due to cold electrons; in addition it would reduce electron drag.[18,20] In conclusion, density of the migma plasma was increased to $n_v \sim 10^9$ and $n_c \sim 10^{10}$ cm^{-3} (limited by the injected ion current $\leqslant 0.5$ mA) without the destructive instabilities observed in thermal plasmas at several orders-of-magnitude lower n_v which, in turn, led to the abandonment of simple mirror confinement in the 1960's, and without occurrence of the predicted $m=1$ flute instability. These stabilizing properties we attribute to the large r_L and small P_θ. If, with a higher current injection, the stability properties hold at higher n, the migma diamagnetic well[21] could offer better confinement of megaelectronvolt ions than more complex geometries.

[a]Permanent address: Polytechnic Institute of New York, Brooklyn, N. Y. 11201.

[b]Visiting scientist at Polytechnic Institute of New York from the Institute of Radio Engineering, Chendu, Sichuan, P. R. China.

[1]H. Postma *et al.*, Phys. Rev. Lett. **16**, 265 (1966).

[2]J. L. Dunlap *et al.*, Phys. Fluids **9**, 199 (1966).

[3]M. N. Rosenbluth *et al.*, Nucl. Fusion Suppl. Pt. 1, 143 (1962).

[4]A. B. Mikhailovskii, *Instabilities of an Inhomogeneous Plasma,* Theory of Plasma Instabilities, Vol. 2 (Plenum, New York, 1974), p. 125.

[5]L. G. Kuo *et al.*, Phys. Fluids 7, 988 (1964).

[6]W. Bernstein *et al.*, in *Proceedings of the Second International Conference on Plasma Physics and Controlled Nuclear Fusion Research, Culham, England, 1965* (International Atomic Energy Agency, Vienna, Austria, 1966), p. 23.

[7]L. G. Kuo *et al.*, J. Nucl. Energy **C6**, 505 (1964).

[8]A. H. Futch *et al.*, in *Proceedings of the Second International Conference on Plasma Physics and Controlled Nuclear Fusion Research, Culham, England, 1965* (International Atomic Energy Agency, Vienna, Austria, 1966), p. 3.

[9]M. Emery, Bull. Am. Phys. Soc. **22**, 649 (1977).

[10]B. Maglich *et al.*, Phys. Rev. Lett. **27**, 909 (1971), and Appl. Phys. Lett. **26**, 609 (1975).

[11]J. Ferrer *et al.*, Nucl. Instrum. Methods **157**, 269 (1978). For *n* distributions see Fig. 9.

[12]F. Gratton, Atomkernenergie **32**, 121 (1978).

[13]B. Maglich *et al.*, Nucl. Instrum. Methods **120**, 309 (1974).

[14]S. C. Menasian *et al.*, Nucl. Instrum. Methods **144**, 49 (1977).

[15]J. Ferrer *et al.*, Nucl. Instrum. Methods **144**, 51 (1977).

[16]*Semi-Annual Progress Report, Dec. 1982,* edited by S. Menasian (United Sciences, Inc., Princeton, New Jersey, 1982).

[17]R. A. Miller, Phys. Rev. Lett. **29**, 1590 (1972).

[18]J. G. Cordey, *et al.*, in *Proceedings of the Third International Conference on Plasma Physics and Controlled Nuclear Fusion Research, Novosibirsk, U.S.S.R., 1968* (International Atomic Energy Agency, Vienna, Austria, 1969).

[19]R. A. Miller, Nucl. Instrum. Methods **119**, 275 (1974).

[20]J. R. McNally, Nucl. Fusion **11**, 191 (1971).

[21]S. R. Channon, J. Golden, and R. A. Miller, Phys. Rev. A **17**, 407 (1968).